buildings

MDPI

Article

Fire-Resistant Steel Structures: Optimization Mathematical Model with Minimum Predicted Cost of Fire Protection Means

Marina Gravit [1,*], Anton Radaev [1], Nikita Shcheglov [1], Natalia Konstantinova [2] and Alla Tsepova [1]

[1] Peter the Great St. Petersburg Polytechnic University, Saint-Petersburg 195251, Russia; radaev_ae@spbstu.ru (A.R.); tsheglov.ne@edu.spbstu.ru (N.S.); allatsepova@mail.ru (A.T.)
[2] FGBU VNIIPO of EMERCOM of Russia, VNIIPO District, 12, Balashiha 143903, Russia; konstantinova_n@inbox.ru
* Correspondence: gravit_mv@spbstu.ru

Abstract

Steel structures quickly lose stability during a fire, which is why fire protection measures are used to increase their fire resistance limits. Structural fire protection in the form of boards or covers can achieve structural stability values ranging from 30 to 240 min under various fire conditions. Structural fire protection has certain advantages—it does not change its geometry during a fire, its behavior is predictable during testing (unlike intumescent fire protection), it has broad climatic applicability, and it can achieve high fire resistance limits. This article presents a mathematical model that calculates the minimum cost of structural fire protection while ensuring that the unexposed side of a steel column does not exceed 500 °C and achieves 180 min of standard fire resistance. Optimal values were extracted using genetic algorithms in the MS Excel environment and the "Solver" tool. The model was tested on a sample of 39 structural materials, such as cement boards, covers, and enclosures. The calculated coefficient of determination (R^2) for the predictive model of the main component was 0.948. The predicted material cost was 6.83 \$/m^2. This study's results can be used for preliminary cost estimation of fire protection treatments for steel structures in large design and operating companies.

Keywords: fire safety; steel structures; fire resistance; fire protection; mathematical model; cost of structural fire protection; fire protection treatments; genetic algorithms

1. Introduction

Fire safety measures are one of the most important sections in the concept of general safety of buildings and structures, ensuring the protection of people and the environment from various threats in emergency situations. The strength of the structural systems of fire protection facilities and ensuring their required fire resistance play a fundamental role.

Steel structures lose their fire resistance relatively quickly; their fire resistance limits are 5–15 min, so various fire protection measures are used to increase fire resistance limits.

It is important to note that the use of structural fire protection significantly increases the cost of designing and constructing capital construction projects. To achieve the highest fire resistance ratings of structures, various types of structural fire protection are used. Mineral wool is widely applied in indoor environments, ceramic fiber linings are commonly used in tunnels, and cement boards, due to their good moisture resistance, are suitable for outdoor applications, such as overpasses and facilities in the oil and gas industry (Figure 1).

Check for updates

Academic Editor: Flavio Stochino

Received: 30 October 2025
Revised: 21 December 2025
Accepted: 23 December 2025
Published: 2 January 2026

Copyright: © 2026 by the authors. Licensee MDPI, Basel, Switzerland. This article is an open access article distributed under the terms and conditions of the Creative Commons Attribution (CC BY) license.

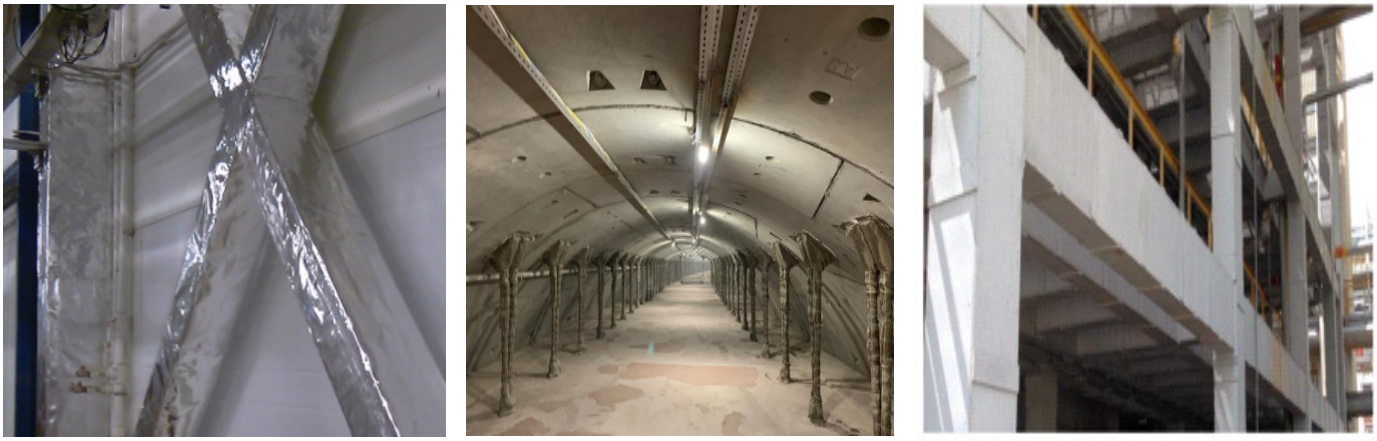


Figure 1. Examples of structural fire protection used in the model.

1.1. The Nominal Temperature—Time Curves and Fire Protection

To understand the resistance of such structures to fires, standard testing methods are carried out under the cellulose fire mode according to ISO 834 [1] (the fundamental world standard for fire resistance testing, which is why this mode is also called "standard" (S)). Modern software packages implementing a field fire model also simulate the "real" fire mode, which can be obtained based on the combustible load at the facility [2,3]. As can be seen from Figure 2, under the standard temperature mode, the temperature increases according to a logarithmic curve; after 5 min, the heat flow is 25 kW/m^2 [4]. Figure 3 shows a graph of the combustion mode of hydrocarbons and the fire resistance curves of steel plates under this mode; the heat flow is 50 kW/m^2 [5].

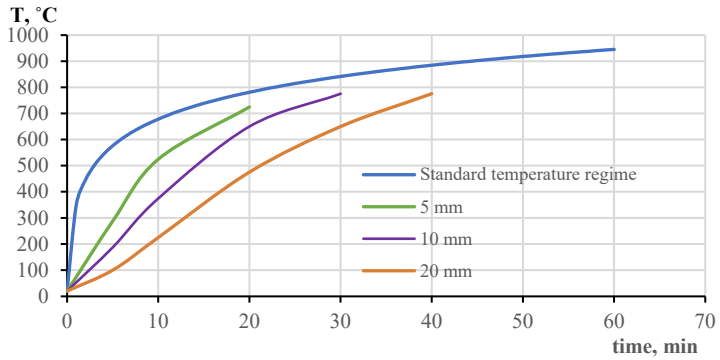


Figure 2. Temperature–time curves and rate of temperature increase for unprotected steel plates of different thickness, according to the standard curve (wood combustion) [6].

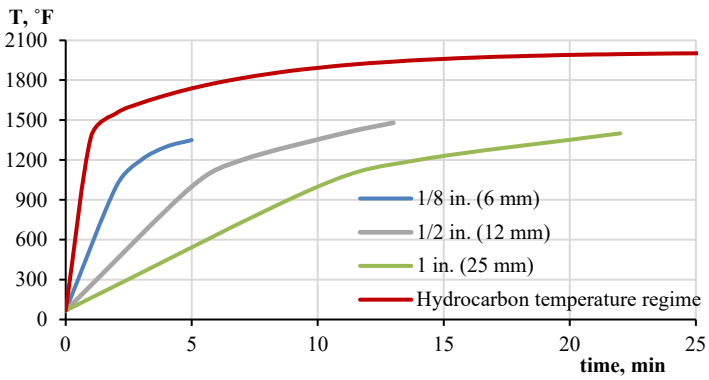


Figure 3. Temperature–time curves and the rate of temperature increase for unprotected steel plates of different thicknesses exposed to an open gasoline fire along the hydrocarbon combustion curve [6].

The hydrocarbon fire mode (H-mode) is used to protect building structures in the oil and gas complex, chemical complex, and tunnel structures.

Without passive fire protection (PFP), steel structures have a fire resistance of only 8–25 min at a critical temperature of 500 °C for steel [1], according to the S-fire curve. Therefore, PFP is typically used to protect steel structures [6]. Figure 4 shows the types of fire protection coatings used in capital construction projects.

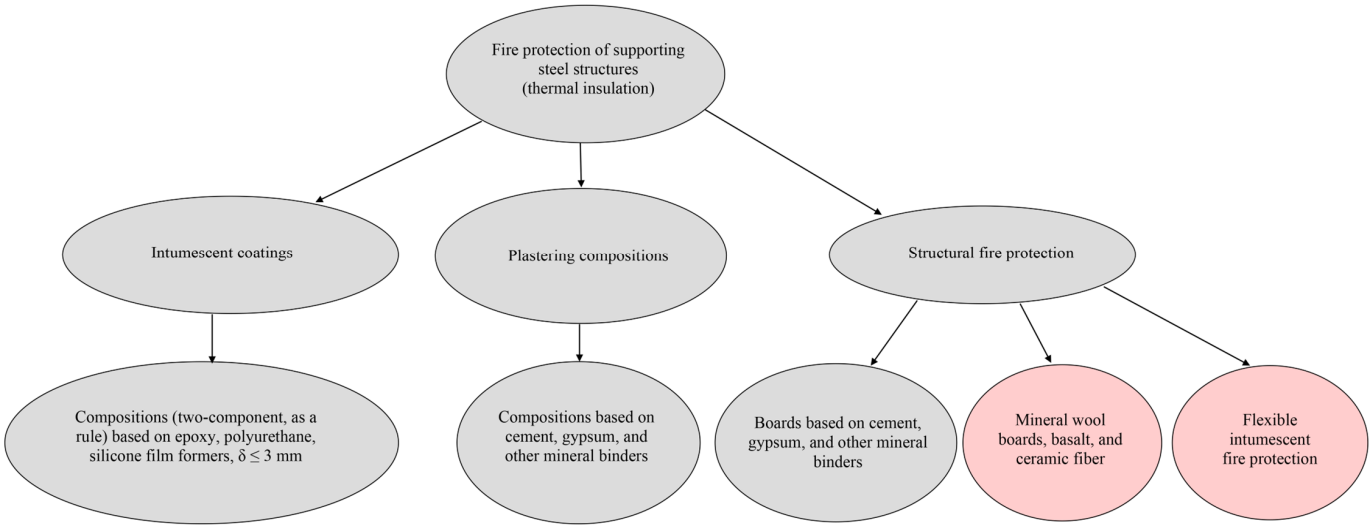


Figure 4. Schematic of fire protection coatings applied at capital construction projects.

The fire protection samples in the optimization model were samples of structural fire protection: mineral wool, boards, and basalt (In Figure 4 they are shown in pink). These materials are least susceptible to changes in their physical characteristics during exposure to fire.

1.2. Limit States of Structures and Predictive Model with Fire Protection

Fire resistance is defined as the ability of a specified structure (considering its material properties and geometry) to maintain its required load-bearing and/or fire-separating functions under designated fire exposure conditions for a specified duration. The load-bearing capacity (R) is compromised when steel reaches critical temperatures of 450–500 °C, according to [1–9], or 538 °C, as per [5]. The fire-separating function depends on both thermal insulation criteria (I), measured as an average of 140 °C temperature on the unexposed surface via thermocouples, and integrity criteria (E), which involve crack formation and material detachment that are analytically challenging to quantify [1,8,9]. The fire resistance limit represents either the duration until any single failure criterion (R, E, or I) is met or until the simultaneous occurrence of multiple failure modes.

For unprotected steel structures, fire resistance can be calculated analytically using either the section factor (A_p/V—the ratio of heated surface area to volume), as described in [9], or its inverse value (specific metal thickness), as per [7]. These calculations employ thermophysical equations that account for heat transfer mechanisms (convection, radiation, and conduction) based on standardized fire curves while incorporating temperature-dependent variations in the thermal properties of fire protection materials.

Fire protection properties are studied in a comparative setting relative to unprotected steel structures. For example, in [7], a volume factor is used for a 1.7 m high steel structure coated with fire protection and subjected to a temperature of 500 °C. Several such structures are considered in standards [10], and fire protection is also studied in a comparative context with other types of fire protection and with unprotected structures [11].

Figure 5 shows examples of fire protection efficiency studies of structural fire protection measures according to the standard [7]. The volumetric coefficient of such coatings is A_p/V = 130 mm^{-1} and the column height is 1.7 m. Thermocouples are located at three points. The structural fire protection measures presented are used in the initial data set in this article.



Figure 5. An example of the arrangement of thermocouples and a view of a sample without fire protection and with different structural fire protection.

1.3. Review of Research on Predicting the Fire Resistance of Structures Under Different Fire Exposure

Currently, digital technologies use a variety of algorithms and methods based on optimization and modeling methods, including the fire resistance of structures. The use of mathematical modeling methods for predicting the fire resistance of structures has been discussed in numerous studies [12–14].

For example, article [15] presents the results of parametric studies to develop a simplified equation for assessing the fire resistance of reinforced concrete columns under biaxial bending conditions. The proposed equation accounts for the effects of spalling caused by non-uniform fire exposure, biaxial loading, and design fire scenarios. The equation's reliability is established by comparing its predictions with finite element analysis results and experimental test data.

Article [16] describes the challenges of predicting structural performance in fires, with a view to the past, the present, and the future. Despite the huge advances in computational capability for both fire modelling and structural analysis, it remains very difficult to give accurate predictions of structural performance in a single building with a known fire. In this work [17], a parametric study of a ten-story steel-framed building exposed to fire is presented, evaluating six different parameters: fire intensity, fire spread, load paths, temperature-induced creep, local instability, and analysis method. The results of validated finite element models are used to assess the influence of various parameters and recommend critical parameters for inclusion in the analysis.

Article [18] proposes a modified cost optimization objective function that simplifies reliability target assessments and reduces the number of assumptions. The optimal safety level is expressed as a function of a new dimensionless variable called the "Damage Investment Index" (DII). The cost optimization approach is verified against reliability targets for normal design conditions. This method is then applied to evaluate DII and corresponding optimal reliability indicators for fire-exposed structures. Two practical examples are presented: a one-way loaded reinforced concrete slab and an axially loaded steel column.

The authors conducted work on solving problems of optimizing enclosing structures using genetic algorithm methods [19,20]. Requirements for the energy efficiency of residential buildings and the heat transfer characteristics of structural layers were taken into account [21–24].

Analytical and numerical methods for predicting fire resistance, as well as corresponding experimental results for thin floor beam (SFB) structures as floor systems under fire conditions, are presented in [25]. It is established that further research is needed in compliance with the requirements of European standards so that the construction industry can take advantage of composite methods while meeting safety requirements.

In their study [26], the authors used six new approaches to artificial intelligence for masonry. The study examined key parameters determining tensile strength and identified complex relationships often overlooked by traditional models. Among AI models, ensemble learning methods demonstrate impressive generalization performance.

The authors [27] conducted a detailed mechanical and seismic analysis of the structure before and after optimization using a genetic algorithm. The results showed that the optimized design meets various requirements, such as strength, stiffness, stability, and seismic resistance. Material consumption was reduced by approximately 12% and concrete consumption by approximately 8%, significantly reducing construction costs.

The study [28] considers a design optimization methodology that includes generating truss parameters using Dynamo software (Version: 3.0.4); performing a reliability analysis that includes finite element analysis (FEM) as a limit state function and using FEM to achieve optimal design approaches and a conservative model in Robot Structural Analysis 2024 (RSA) software in real time for further adjustment. The results of the study show that workflow optimization using a BIM environment can improve the design process.

This article presents a mathematical model that reduces the minimum cost of a structural fire protection system, maintains a constant temperature of the unheated surface of a steel column (under the fire protection system) below 500 °C, and achieves a fire resistance limit of 180 min. Optimal values were obtained using genetic algorithms in MS Excel and the Solver tool. Structural fire protection (Figure 1) offers several advantages over other fire protection methods: it does not change its geometric dimensions (thickness) during a fire, exhibits relatively stable performance during testing (unlike intumescent fire protection), has established climatic applicability, and enables it to exceed high fire resistance limits. The model aims to substantiate the characteristics (layer thickness, thermal conductivity, density, and heat capacity) that ensure the required fire resistance performance of the structure under consideration while minimizing the overall material cost.

2. Materials and Methods

The problem of evaluating (or assigning) fire resistance limits for structures is generally formulated as follows and consists of several subtasks:

- Modeling the development of a "real" fire scenario. Based on fire development scenarios, the predicted spread radius of flammable hydrocarbons and heat flux parameters are calculated; currently, field fire models are used for these purposes, though for external applications (fire development in open areas rather than indoors), certain assumptions must be made;
- Solving the static problem for load-bearing structures, considering their thermal heating up to critical temperatures;
- Ensuring the required fire resistance limit under design fire load conditions and calculating the necessary and sufficient amount of fire protection to maintain the structure's fire resistance based on the loss of parameters established in the design documentation.

Loads on the structure are taken in accordance with [29], as for a special combination of loads. The values of loads in the calculation are taken to be equal to their standard values (with safety factors for the load equal to 1.0). The value of the additional coefficient for the operating conditions of the special limit state for steels should be taken as 1.1; the

calculation of the bearing capacity of the steel structure and fastening units is performed according to [30].

The design resistance of steel by yield strength during heating is as follows:

$$R_{yn} = \frac{R_{yn}}{\gamma_t}, \quad (1)$$

where γ_t is the temperature coefficient of reduction of the yield strength of steel upon heating and R_{yn} is the yield strength of steel.

The modulus of elasticity of steel when heated is as follows:

$$E_t = \frac{E}{\gamma_e}, \quad (2)$$

where γ_e is the temperature coefficient of reduction of the elastic modulus of steel upon heating and E is the elastic modulus of steel.

The critical heating temperature of the cross-section (°C), in terms of load-bearing capacity loss, is determined by the smallest value of coefficients γ_t and γ_e. The coefficient γ_e is determined when calculating according to the II-nd limit state, considering the structural limitation of deflection of structural elements under fire exposure.

When determining stresses using calculation complexes, the coefficient γ_t may be determined as follows:

$$\gamma_t = \frac{\sigma_n}{R_{yn}}, \quad (3)$$

where σ_n represents stresses based on the results of the static calculation.

The coefficient γ_e is defined as follows:

$$\gamma_e = \frac{f}{f_u}, \quad (4)$$

where f is the greatest deformation in the element that occurs when calculating the structure from a combination of loads and f_u is the ultimate deflection (deformation) in the element, in accordance with the requirements of SP 20.13330 [29].

The calculation method for determining the temperature of unprotected steel structures in both standard fire conditions consists of a step-by-step calculation using the following relationship:

$$t_{rod,\Delta\tau} = \frac{\Delta\tau}{\lambda_{st} \cdot \delta_{eff} \cdot (C_{st} + D_{st} t_{st})} \cdot \alpha \cdot (t_{g,\tau} - t_{rod}) + t_{rod} \quad (5)$$

where:

$t_{rod,\Delta\tau}$—the temperature of the steel rod after a calculated time interval $\Delta\tau$ (°C);

t_{rod}—the rod temperature at a given moment in time τ (°C);

$t_{g,\tau}$— the rod temperature at a given moment in time τ (°C);

α—the heat transfer coefficient from the heating medium to the surface of the structure (W/(m^2·°C));

C_{st}—the specific heat capacity of steel (J/(kg·°C));

D_{st}—the coefficient of change of C_{st} during heating (J/(kg·°C^2));

λ_{st}—the specific gravity of metal (kg/m^3);

δ_{eff}—the reduced thickness of the metal, m, determined by the following formula:

$$\delta_{eff} = \frac{F}{P}, \quad (6)$$

where:

F—the cross-sectional area of the rod (m^2);

P—the perimeter of the heated surface (m).

The heat transfer coefficient α in the S-mode is determined by the following formula:

$$\alpha = \alpha_k + \alpha_l = 29 + 5.77 \cdot S_{eff} \frac{\left(\frac{T_g}{100}\right)^4 - \left(\frac{T_0}{100}\right)^4}{T_g - T_0}, \quad (7)$$

where:

S_{eff}—the reduced emissivity of the system "fire chamber—structure surface";

T_g—the oven temperature corresponding to time τ (°C);

T_0—the temperature in the oven before the start of thermal exposure (taken equal to the ambient temperature) (°C).

Reduced emissivity is determined by the following formula:

$$S_{eff} = \frac{1}{\frac{1}{S_g} + \frac{1}{S_0} - 1}, \quad (8)$$

where:

S_g—the emissivity of the fire chamber environment;

S_0—the emissivity of the steel rod surface.

In the absence of reference data on the actual values of the physical quantities, the following data are used in the calculation:

$\Delta\tau$ = 0.1 min; λ_{st} = 7850 kg/m^3—at temperature 20–800 °C;

C_{st} = 0.441 kJ/kg·°K; D_{st} = 0.000479 kJ/kg·°K^2; S_g = 0.85; and S_0 = 0.69.

In EN 1993-1-2 [31], the calculation for the fire resistance of steel elements is reduced to determine the increase in temperature of the steel structure over time under nominal temperature conditions, which is then compared with the results obtained using the critical temperature of the steel. In addition to the A_p/V coefficient (in Russian standards, the reduced thickness t_{red} [17]), the heating of the protected profiles depends on the nature of heat transfer (convection, radiation, or thermal conductivity), as well as on the geometric, physical, and thermal properties of the protective material.

In the case of uniform temperature distribution in the cross section, the increase in temperature $\Delta\theta_{\alpha,t}$ of an unprotected steel structure over a time interval Δt is determined from the following expression [32]:

$$\Delta\theta_{\alpha,t} = k_{sh} \cdot \frac{A_m}{V \cdot c_a \cdot \rho_a} \dot{h}_{net} \cdot \Delta t \quad (9)$$

where:

k_{sh}—the correction factor to account for the influence of the shadow effect;

A_m/V—the cross-section coefficient for unprotected steel structures (1/m);

c_a—the specific heat capacity of steel (J/(kg·°C));

$\dot{h}_{net}$—the calculated value of specific heat flow per unit area (W/m^2);

Δt—the period of time (s);

ρ_a—the density of steel (kg/m^3).

Absorbed heat flow $\dot{h}_{net}$ on the heated surfaces is determined by taking into account convection and radiation heat exchange, as follows:

$$\dot{h}_{net} = \dot{h}_{net,c} + \dot{h}_{net,r} \quad (10)$$

where:

$\dot{h}_{net,c}$—the specific heat flow determined by convection;

$\dot{h}_{net,r}$—the specific heat flow determined by radiation.

The convection component of the absorbed heat flow is as follows:

$$\dot{h}_{net,c} = \alpha_c \cdot (\theta_g - \theta_m) \tag{11}$$

where:

θ_g—the temperature near the steel structure (the temperature of one of the nominal fire modes) (°C).

—S-regime:

$$\theta_g = 345 \cdot \lg(8 \cdot t + 1) + T_0, \tag{12}$$

where:

θ_m— the surface temperature of steel structure (°C);

α_c—the convection heat transfer coefficient equal to:

—at S-regime—25 W/(m^2·°C).

The thermal flow of radiation per unit area of the surface of the structure $\dot{h}_{net,r}$ is determined by the following formula:

$$\dot{h}_{net,r} = \Phi \cdot \varepsilon_f \cdot \varepsilon_m \cdot \sigma \cdot ((\theta_r + 273)^4 - (\theta_m + 273)^4) \tag{13}$$

where:

Φ—the slope coefficient, equal in most cases to 1;

ε_f—flame emissivity, assumed as 1;

σ—the Stefan–Boltzmann constant: 5.67 × 10^{-8} W/ (m^2·°C^4);

θ_m—the temperature of the steel structure's surface (°C);

ε_m—the surface absorptivity of the steel structure: 0.7 (for carbon steel);

θ_r—the effective fire radiation temperature (when the structure is heated from all sides $\theta_r = \theta_g$) (°C).

The temperature increases ($\Delta\theta_{\alpha,t}$) over time interval Δt are determined using the following formula [32]:

$$\Delta\theta_{\alpha,t} = \frac{\lambda_p \cdot \frac{A_p}{V}}{d_p \cdot c_a \cdot \rho_a} \cdot \frac{(\theta_{g,t} - \theta_{a,t})}{(1 + \frac{\varphi}{3})} \cdot (e^{\frac{\varphi}{10}} - 1) \cdot \Delta\theta_{g,t} \tag{14}$$

where:

$$\varphi = \frac{c_p \cdot \rho_p}{c_a \cdot \rho_a} \cdot d_p \cdot \frac{A_p}{V} \tag{15}$$

A_p/V—the section ratio (m^{-1});

c_p—the specific heat capacity of fire-protective material (J/(kg·°K));

d_p—the thickness of fire protection material (m);

Δt—the period of time (s), no more than 30 s;

$\theta_{a,t}$—the temperature of steel at time t (°C);

$\theta_{g,t}$—the ambient temperature at time t (°C);

$\Delta\theta_{g,t}$—the increase in ambient temperature over a period of time Δt (°C);

λ_p—the coefficient of thermal conductivity for fire protection (W/(m·°K));

ρ_a—the density of the fireproof material (kg/m^3).

The calculation formula for $\theta_{a,t}$ does not take into account the effect of water contained in "wet" fire protection materials and absent in the so-called "dry" fire protection materials [32]; the heat-insulating properties of the latter depend on the mass specific heat capacity c_p, density ρ, and thermal conductivity λ. Of course, these values depend on the

temperature θ; therefore, the fire protection material is characterized by three curves: $c_p - \theta$, $\rho - \theta$ and $\lambda - \theta$. In addition, the radiation on the protected surface depends on the type of material and the method of its application.

Thus, the thermophysical properties of the materials can be reduced to a single coefficient, which can be called the coefficient of "conditional (or effective) thermal conductivity"—γ. Then, the thermal resistance of the protective layer, with an average thickness e, is e/γ.

$$\Delta\theta_\alpha = \frac{1}{\frac{1}{K} + \frac{e}{\gamma}} \cdot \frac{S}{V} \cdot \frac{1}{C \cdot p_a \cdot \rho_a} \cdot (\theta_f - \theta_\alpha) \cdot \Delta t \quad (16)$$

Thermophysical characteristics were calculated according to the inverse heat conduction problem. The relationship between time t_1 required to reach a certain temperature in a steel element with a massiveness coefficient $\left(\frac{s}{V}\right)_1$, with fire protection of thickness e_1 and time t_2 required to reach the same temperature in a steel element with massiveness coefficient $\left(\frac{s}{V}\right)_2$, protected by a layer of the same protective material with thickness e_1, is determined using the following expression (18) [32]:

$$\frac{t_1}{t_2} = \left\{ \frac{e_1}{e_2} \cdot \frac{\left(\frac{s}{V}\right)_2}{\left(\frac{s}{V}\right)_1} \right\}^{0.8} \quad (17)$$

3. Discussion and Results

The objective of this modeling is structural fire protection on a steel structure that does not change its geometric parameters or its density (as an assumption) when exposed to temperature for 180 min (failure to achieve T = 500 °C in the steel structure [33]). A nonlinear programming problem with a nonlinear objective function and a region of admissible solutions determined by nonlinear constraints was solved [34]. The mathematical description of the problem is as follows [35]:

$$C_\Sigma(\{x_j\}) \rightarrow \min \quad (18)$$

$$x_j^{\min} \leq x_j \leq x_j^{\max}, j = 1, 2, \ldots, n \quad (19)$$

$$\theta_a(\{x_j\}, t_{req}) \leq \theta_a^{\max} \quad (20)$$

where C_Σ represents the total cost of fireproofing material in conventional units (c.u.) and x_j represents the unknown variable—a characteristic value of fireproofing material with index j (j = 1, 2, …, n); taking into account the previously introduced designations.

The set of characteristics λ_p, d_p, and c_p for fire protection materials under specified technical constraints belongs to a domain where:

$$\{\lambda_p, d_p, c_p, p_p\} \subset \{x_{j=1}, x_{j=2}, \ldots, x_{j=n}\} \quad (21)$$

where:

n—the total number of considered protective material characteristics, units;

$x_j^{\min}$, $x_j^{\max}$—the minimum and maximum values of the fireproofing material characteristic with index j [35];

t_{req}—the standard time interval for maintaining the structure's operational state under fire exposure (time to reach 500 °C on the unexposed side), min;

θ_a—the structure temperature value determined by the material characteristics and the time factor value (°C);

$\theta_a^{\max}$—the maximum allowable temperature of the structural material at which it maintains its operational capacity (°C).

The optimal values of the unknown variables $\{x_j\}$ can be determined by implementing the mathematical model described by expressions (19–26), with known dependencies $C_\Sigma(\{x_j\})$ and $\theta_a(\{x_j\}, t_{req})$, using an evolutionary (genetic) algorithm [35].

If the model of dependence of the total cost of fireproofing material on the material characteristics values $C_\Sigma(\{x_j\})$ can be formed based on the analysis of various instances of fireproofing materials available for mass application within fire protection solutions for building structures, then the formation of the model of dependence of the structural material temperature value on the aforementioned technical characteristics values, as well as the time factor $\theta_a(\{x_j\}, t_{req})$, requires planning and conducting a sufficiently large number of experiments in the field of structural fire resistance and, consequently, significant amounts of labor, financial, and other resources will be involved, especially in the case of H-mode modeling.

The problem of the objective function and system of constraints of nonlinear optimization (nonlinear programming problem) was solved [35].

To solve the optimization problem, the "Solver" tool built into the MS Excel environment was used [34]. Fragments of the worksheets "Calculation" in the "Microsoft Excel" file, corresponding to the presentation of initial data, parameters, and characteristics of the optimization model, and the presentation of the main matrix of equation systems for the main calculated characteristics of the optimization model, are given in the Supplementary Materials.

Depending on the nature of the thermal exposure, as well as the nature of influence on the specific cost of fireproofing material, its technical characteristics are divided into the following categories:

- s^I: main (primary) technical characteristics describing the state of fireproofing material at the onset of fire, not directly describing changes in the material properties during fire development, and characterized by relatively high influence on the material's specific cost;
- s^{II}: additional (secondary) technical characteristics of the material, directly describing changes in the fireproofing material properties during fire development, characterized by relatively low influence on the material's specific cost.

The main and additional technical characteristics of the material form the main and additional components of the material's specific cost, respectively, whose superposition determines the actual specific cost of the material.

As an objective function, we consider the dependence function of specific cost on the main characteristics of the thermal insulation material. The mathematical model is described by the following expression:

$$\widetilde{y}^{\mathrm{I(II)}} = s^{\mathrm{I(II)}}_{p=0} + \sum_{j^{\mathrm{I(II)}}=1}^{n^{\mathrm{I(II)}}} \left(s^{\mathrm{I(II)}}_{p=j^{\mathrm{I(II)}}} \cdot x_{j^{\mathrm{I(II)}}} + s^{\mathrm{I(II)}}_{p=n^{\mathrm{I(II)}}+j^{\mathrm{I(II)}}} \cdot x^2_{j^{\mathrm{I(II)}}} \right) \tag{22}$$

where:

$\widetilde{y}^{\mathrm{I(II)}}$—the predicted value of the specific cost of the fireproofing material (CU/m^2);

n—the number of technical characteristics for the fireproofing material, determining its specific cost (units);

$s^{\mathrm{I(II)}}_{p=0}$—a component of the specific cost.

The objective function is formed based on statistical data for variants of fireproofing material using the least squares method.

The least squares method involves determining parameters $s_0, s_1, \ldots, s_n$ of the dependence that ensure the minimum value of the sum (across material variants) of squared deviations between the predicted and actual values of the specific cost.

In general, the solution to the parameter determination problem using the least squares method is numerical and obtained by constructing and implementing a separate (local) nonlinear optimization model.

The optimization model is defined by the following expressions:

$$\begin{cases} s^{\mathrm{I}}_{p=0} + \sum\limits_{j^{\mathrm{I}}=1}^{n^{\mathrm{I}}} \left(s^{\mathrm{I}}_{p=j^{\mathrm{I}}} \cdot x_{j^{\mathrm{I}}} + s^{\mathrm{I}}_{p=n^{\mathrm{I}}+j^{\mathrm{I}}} \cdot x^2_{j^{\mathrm{I}}} \right) + s^{\mathrm{II}}_{p=0} + \sum\limits_{j^{\mathrm{II}}=1}^{n^{\mathrm{II}}} \left(s^{\mathrm{II}}_{p=j^{\mathrm{II}}} \cdot x_{j^{\mathrm{II}}} + s^{\mathrm{II}}_{p=n^{\mathrm{II}}+j^{\mathrm{II}}} \cdot x^2_{j^{\mathrm{II}}} \right) \to \min; & (23) \\ \min\limits_i \{x_{ij}\} \le x_j \le \max\limits_i \{x_{ij}\}, \ j = 1, 2, \ldots, n; & (24) \\ \min\limits_i \left\{ \dfrac{x_{ij}}{x_{ij'}} \right\} \cdot x_{j'} \le x_j \le \max\limits_i \left\{ \dfrac{x_{ij}}{x_{ij'}} \right\} \cdot x_{j'}, \ j = 2, 3, \ldots, n; \ j' = 1, 2, \ldots, j-1; & (25) \\ \theta_{a\ k=N}(\{x_j\}) \le \theta_a^{\max}. & (26) \end{cases}$$

The name of the accounted technical characteristic of the fireproofing material; structural parameters, indices, initial data, and unknown variables of the optimization model; and calculated characteristics of the optimization model are presented in Tables 1–3 and in the Supplementary Materials, respectively.

Table 1. The physical and technical characteristics of the material.

Index	Name of the Accounted Technical Characteristic of the Fireproofing Material	Unit	Notation
j	-	$\mathrm{MU_{x\,j}}$	x_j
1	Thickness of fire protection material	m	δ
2	λ at 20 °C	W/(m·°K)	λ_0
3	Increment coefficient of λ20 to λ300	-	λ_1/λ_0
4	Increment coefficient of λ300 to λ500	-	λ_2/λ_1
5	Specific heat capacity at 20 °C	J/(kg·°K)	c_0
6	Increment coefficient of C00 at 300 °C to C11 at 20 °C	-	c_1/c_0
7	Increment coefficient of specific heat capacity at 300 °C relative to 500 °C	-	c_2/c_1
8	Material density	$\mathrm{kg/m^3}$	ρ

Table 2. The structural parameters, indices, input data, and unknown variables of the optimization model.

No.	Name of Model Structure Parameter/Index/Input Data Element	Unit	Notation/ Expression
1	Quantities:		
1.1	Number of technical characteristics of fireproofing material	unit	n
1.2	Main (additional) characteristics determining the main (additional) component of specific cost (1)	unit	$n^{\mathrm{I(II)}}$
1.3	Parameters for the predictive model for the main (additional) component of specific cost (2)	unit	$z^{\mathrm{I(II)}}$
1.4	Number of fireproofing material instances	unit	m
2	Indices and Sets:		
2.1	Index of fireproofing material instance	-	$i = 1, 2, \ldots, m$
2.2	Index of fireproofing material technical characteristic	-	$j = 1, 2, \ldots, n$
2.3	Index of the main (additional) technical characteristic of fireproofing material (3)	-	$j^{\mathrm{I(II)}} = 1, 2, \ldots, n^{\mathrm{I(II)}}$
2.4	Index of the predictive model parameter for the main (additional) cost component	-	$p = 0, 1, \ldots, z^{\mathrm{I(II)}} - 1$
2.5	Index of time moment (4)	-	$k = 1, 2, \ldots, N$
2.6	Set of indices for the main technical characteristics of the material	-	$J^{\mathrm{I}} = \left\{ j \mid \zeta_j = 1 \right\}$
2.7	Set of indices for the additional technical characteristics of the material	-	$J^{\mathrm{II}} = \left\{ j \mid \zeta_j = 0 \right\}$

Table 2. *Cont.*

No.	Name of Model Structure Parameter/Index/Input Data Element	Unit	Notation/ Expression
3	Input Data		
3.1	General Input Data		
3.1.1	Share of the main component in the total specific cost of the material	-	γ
3.1.2	Cross-section coefficient of the insulated structure	m^{-1}	A_p/V
3.1.3	Specific heat capacity of the structural material	J/(kg·°K)	c_a
3.1.4	Density of the structural material	kg/m^3	ρ_a
3.1.5	S-mode exposure duration	s	T
3.1.6	Time interval duration	s	Δt
3.1.7	Maximum allowable temperature for the structural material	m^{-1}	θ_a^{max}
3.1.8	Reference temperature for the approximation curve (index 0)	°C	θ_0
3.1.9	Reference temperature for the approximation curve (index 1)	°C	θ_1
3.1.10	Reference temperature for the approximation curve (index 2)	°C	θ_2
3.2	Input Data for Each Fireproofing Material Variant (index i = 1, 2, . . ., m)		
3.2.1	Material name	-	-
3.2.2	Actual specific cost value	CU/m^2	y_i
3.3	Input Data for Each Technical Characteristic (index j = 1, 2, . . ., n) per Material Variant (index i = 1, 2, . . ., m)		
3.3.1	Value of the technical characteristic	$MU_{x\,j}$	x_{ij}
4	Unknown Variables		
4.1	Variables considered for each technical characteristic with index j (j = 1, 2, . . ., n)		
4.1.1	Value of the technical characteristic	$MU_{x\,j}$	x_j

Note: (1) The relationship between input data elements and those defined in Table items 2.6 and 2.7 is determined by the expression: $n^{\mathrm{I(II)}} = \left|J^{\mathrm{I(II)}}\right|$; (2) The relationship between input data elements and the element defined in Table item 1.2 is determined by the expression: $z^{\mathrm{I(II)}} = 2{\cdot}n^{\mathrm{I(II)}} + 1$; (3) The correspondence between indices in Table items 2.2 and 2.3 is described by the expressions (Supplementary Materials); (4) The maximum index value is determined by the expression specified in Table 3, item 6.18.

Table 3. Calculated Characteristics of the Optimization Model.

No.	Name of Model Structure Parameter/Index/Input Data Element		Unit	Expression
1	Calculated characteristics for each technical characteristic with index j (j = 1, 2, . . ., n) j (j = 1, 2, . . ., n)			
1.1	Structurally permissible limit value of the characteristic	minimum	$MU_{x\,j}$	$x_j^{\min} = \min\limits_i\left\{x_{ij}\right\}$
1.2		maximum	$MU_{x\,j}$	$x_j^{\max} = \max\limits_i\left\{x_{ij}\right\}$
2.1	Calculated characteristics for each main (additional) technical characteristic with index $j^{\mathrm{I(II)}}$ $\left(j^{\mathrm{I(II)}} = 1, 2, \ldots, n^{\mathrm{I(II)}}\right)$			
2.1.1	Element of the main matrix of the equation system for determining the predictive model parameters, corresponding to row index d $\left(d = 0, 1, \ldots, z^{\mathrm{I(II)}} - 1\right)$ and column index l $\left(l = 0, 1, \ldots, z^{\mathrm{I(II)}} - 1\right)$ (1)		-	$A_{dl}^{\mathrm{I(II)}} = f\left(\left\{x_{ij^{\mathrm{I(II)}}}\right\}\right)$
2.1.2	Element of the partial matrix of the equation system for determining the predictive model parameter with index p $\left(p = 0, 1, \ldots, z^{\mathrm{I(II)}} - 1\right)$, corresponding to row index d $\left(d = 0, 1, \ldots, z^{\mathrm{I(II)}} - 1\right)$ and column index l $\left(l = 0, 1, \ldots, z^{\mathrm{I(II)}} - 1\right)$ (2)		-	$A_{dl}^{\mathrm{I(II)}\ p} = f\left(\left\{x_{ij^{\mathrm{I(II)}}}\right\}\right)$
2.1.3	Main matrix of the equation system for determining the predictive model parameters (3)		-	$\Lambda^{\mathrm{I(II)}} = f\left(\left\{x_{ij^{\mathrm{I(II)}}}\right\}\right)$
2.2	Calculated characteristics for each predictive model parameter of the main (additional) specific cost component with index p $\left(p = 0, 1, \ldots, z^{\mathrm{I(II)}} - 1\right)$			
2.2.1	Partial matrix of the equation system for determining the predictive model parameters (4)		-	$\Lambda_p^{\mathrm{I(II)}} = f\left(\left\{x_{ij^{\mathrm{I(II)}}}\right\}\right)$
2.2.2	Predictive model parameter defining the proportionality between the specific cost value and the technical characteristic value		var. (5)	$s_p^{\mathrm{I(II)}} = \frac{\left\|\Lambda_p^{\mathrm{I(II)}}\right\|}{\left\|\Lambda^{\mathrm{I(II)}}\right\|}$
3	Calculated characteristics for each pair of material technical characteristics with indices j = 2, 3, . . ., n and j' = 1, 2, . . ., $j-1$			
3.1	Maximum allowable conditional characteristic value	minimum	$MU_{x\,j}$	$\tilde{x}_{jj'}^{\min} = \min\limits_i\left\{\frac{x_{ij}}{x_{ij'}}\right\}\cdot x_{j'}$
3.2		maximum	$MU_{x\,j}$	$\tilde{x}_{jj'}^{\max} = \max\limits_i\left\{\frac{x_{ij}}{x_{ij'}}\right\}\cdot x_{j'}$

Table 3. *Cont.*

No.	Name of Model Structure Parameter/Index/Input Data Element		Unit	Expression
4	Calculated characteristics for each fireproofing material variant with index i ($i = 1, 2, \ldots, m$)			
4.1	Predicted specific cost value	Main component	CU/m^2	$y_i^{I} = y_i \cdot \gamma$
4.2		Additional component	CU/m^2	$y_i^{II} = y_i \cdot (1-\gamma)$
4.3	Predicted value of the main (additional) specific cost component		CU/m^2	$\tilde{y}_i^{I(II)} = s_{p=0}^{I(II)} + \sum_{j^{I(II)}=1}^{n^{I(II)}} \left(s_{p=j^{I(II)}}^{I(II)} \cdot x_{ij^{I(II)}} + s_{p=n^{I(II)}+j^{I(II)}}^{I(II)} \cdot x_{ij^{I(II)}}^2 \right)$
4.4	Predicted specific cost value		CU/m^2	$\tilde{y}_i = \tilde{y}_i^{I} + \tilde{y}_i^{II} = s_{p=0}^{I} + \sum_{j^{I}=1}^{n^{I}} \left(s_{p=j^{I}}^{I} \cdot x_{ij^{I}} + s_{p=n^{I}+j^{I}}^{I} \cdot x_{ij^{I}}^2 \right) + s_{p=0}^{II} + \sum_{j^{II}=1}^{n^{II}} \left(s_{p=j^{II}}^{II} \cdot x_{ij^{II}} + s_{p=n^{II}+j^{II}}^{II} \cdot x_{ij^{II}}^2 \right)$
5	Calculated characteristics for each time moment of thermal exposure with index k ($k = 1, 2, \ldots, N$) [6]			
5.1	Time factor value		s	$t_k = \Delta t \cdot (k-1)$
5.2	Ambient temperature parameter at time moment	Current	°C	$\theta_{g\,k} = 345 \cdot \lg\left(8 \cdot \frac{t_k}{60} + 1\right) + 20$
5.3		Next	°C	$\theta_{g\,k+1} = 345 \cdot \lg\left(8 \cdot \frac{t_k + \Delta t}{60} + 1\right) + 20$
5.4	Ambient temperature change		°C	$\Delta\theta_{g\,k} = \theta_{g\,k+1} - \theta_{g\,k}$
5.5	Structural material temperature value		°C	$\theta_{a\,k} = \begin{cases} \theta_{g\,k}, & k = 1; \\ \theta_{a\,k-1} + \Delta\theta_{a\,k-1}, & k > 1 \end{cases}$
5.6	Thermal conductivity coefficient for the fireproofing material [7]		W/(m·°K)	$\lambda_{p\,k} = a_0 + a_1 \cdot (\theta_{a\,k} - \theta_0) + a_2 \cdot (\theta_{a\,k} - \theta_0) \cdot (\theta_{a\,k} - \theta_1)$
5.7	Specific heat capacity for the fireproofing material [8]		J/(kg·°K)	$c_{p\,k} = b_0 + b_1 \cdot (\theta_{a\,k} - \theta_0) + b_2 \cdot (\theta_{a\,k} - \theta_0) \cdot (\theta_{a\,k} - \theta_1)$
5.8	Additional calculation parameter value		-	$\phi_k = \frac{c_{p\,k} \cdot x_{j=8}}{c_a \cdot \rho_a} \cdot x_{j=1} \cdot A_p / V$
5.9	Structural material temperature change		°C	$\Delta\theta_{a\,k} = \frac{\lambda_{p\,k} \cdot A_p / V}{x_{j=1} \cdot c_a \cdot \rho_a} \cdot \frac{\theta_{g\,k} - \theta_{a\,k}}{1 + \frac{\phi_k}{3}} \cdot \Delta t - \left(\exp\left(\frac{\phi}{10}\right) - 1\right) \cdot \Delta\theta_{g\,k}$
6	Generalized Calculated Characteristics of the Model			
6.1	Actual value of the main (additional) specific cost of the fireproofing material	min	CU/m^2	$y^{I(II)\,min} = \min_i \left\{ y_i^{I(II)} \right\}$
6.2		max	CU/m^2	$y^{I(II)\,max} = \max_i \left\{ y_i^{I(II)} \right\}$
6.3	Predicted value of the main (additional) specific cost of the fireproofing material	min	CU/m^2	$\tilde{y}^{I(II)\,min} = \min_i \left\{ \tilde{y}_i^{I(II)} \right\}$
6.4		max	CU/m^2	$\tilde{y}^{I(II)\,max} = \max_i \left\{ \tilde{y}_i^{I(II)} \right\}$
6.5	Calculated coefficient of determination (R^2) for the predictive model of the main (additional) specific cost of fireproofing material		-	$R^{I(II)\,2} = 1 - \frac{\sum_{i=1}^{m} \left(\tilde{y}_i^{I(II)} - y_i^{I(II)} \right)^2}{\sum_{i=1}^{m} \left(y_i^{I(II)} - \frac{\sum_{i=1}^{m} y_i^{I(II)}}{m} \right)^2}$
6.6	Reference point ordinate value for the thermal conductivity approximation curve	0	W/(m·°K)	$\lambda'_0 = x_{j=2}$
6.7		1	W/(m·°K)	$\lambda'_1 = x_{j=2} \cdot x_{j=3}$
6.8		2	W/(m·°K)	$\lambda'_2 = x_{j=2} \cdot x_{j=3} \cdot x_{j=4}$
6.9	Reference point ordinate value for the thermal conductivity approximation curve	0	W/(m·°K)	$a_0 = \lambda'_0$
6.10		1	$W/(m \cdot °K^2)$	$a_1 = \frac{\lambda'_1 - \lambda'_0}{\theta_1 - \theta_0}$
6.11		2	$W/(m \cdot °K^3)$	$a_2 = \frac{1}{\theta_2 - \theta_1} \cdot \left(\frac{\lambda'_2 - \lambda'_0}{\theta_2 - \theta_0} - \frac{\lambda'_1 - \lambda'_0}{\theta_1 - \theta_0} \right)$
6.12	Reference point ordinate value for the specific heat capacity approximation curve	0	J/(kg·°K)	$c'_0 = x_{j=5}$
6.13		1	$J/(kg \cdot °K^2)$	$c'_1 = x_{j=5} \cdot x_{j=6}$
6.14		2	$J/(kg \cdot °K^3)$	$c'_2 = x_{j=5} \cdot x_{j=6} \cdot x_{j=7}$
6.15	Reference point ordinate value for the C approximation curve	0	J/(kg·°K)	$b_0 = c'_0$
6.16		1	$J/(kg \cdot °K^2)$	$b_1 = \frac{c'_1 - c'_0}{\theta_1 - \theta_0}$
6.17		2	$J/(kg \cdot °K^3)$	$b_2 = \frac{1}{\theta_2 - \theta_1} \cdot \left(\frac{c'_2 - c'_0}{\theta_2 - \theta_0} - \frac{c'_1 - c'_0}{\theta_1 - \theta_0} \right)$
6.18	Number of calculated time moments for thermal exposure		units	$N = \frac{T}{\Delta t} + 1$
6.19	Predicted specific cost of the material		CU/m^2	$\tilde{y} = s_{p=0}^{I} + \sum_{j^{I}=1}^{n^{I}} \left(s_{p=j^{I}}^{I} \cdot x_{j^{I}} + s_{p=n^{I}+j^{I}}^{I} \cdot x_{j^{I}}^2 \right) + s_{p=0}^{II} + \sum_{j^{II}=1}^{n^{II}} \left(s_{p=j^{II}}^{II} \cdot x_{j^{II}} + s_{p=n^{II}+j^{II}}^{II} \cdot x_{j^{II}}^2 \right)$

Note: [1] The characteristic is calculated based on the input data element defined in item 3.3.1 of Table 2 using the least squares method (LSM) using the formula (Supplementary Materials). [2] Calculation of the characteristic is performed based on input data elements defined in item 3.3.1 of Table 2, items 2.1, 6.1, 6.2 of Table 2 using the Least Squares Method (LSM) via the formula (Supplementary Materials); [3] Calculation of the characteristic is performed based on the input data element (item 2.1 of Table 3) using the Least Squares Method (LSM) via the formula (Supplementary Materials); [4] The characteristic is calculated based on the input data element (item 2.2 of Table 3) using the least squares method (LSM) according to the formula (Supplementary Materials); [5] The unit of measurement of the calculated characteristic is determined by the index of the parameter of the forecast model and corresponds to "CU/m^2" at, «$CU/(m^2 \cdot MU_{xj}^{I(II)})$» when $p \in \left\{1; 2; \ldots; n^{I(II)}\right\}$, «$CU/((m^2 \cdot MU_{xj}^{I(II)})^{-1/2})$» when $p \in \left\{n^{I(II)} + 1; n^{I(II)} + 2; \ldots; 2 \cdot n^{I(II)}\right\}$; [6] The upper index value is determined by the expression specified in item 5.19 of the table; [7] The calculation of the characteristic is performed based on the results of computing characteristics from items 6.9–6.11 of the table; [8] The calculation of the characteristic is performed based on the results of computing characteristics from items 6.15–6.17 of the table.

The block diagram describing the structure and algorithm of the optimization model is presented in Figure 6.

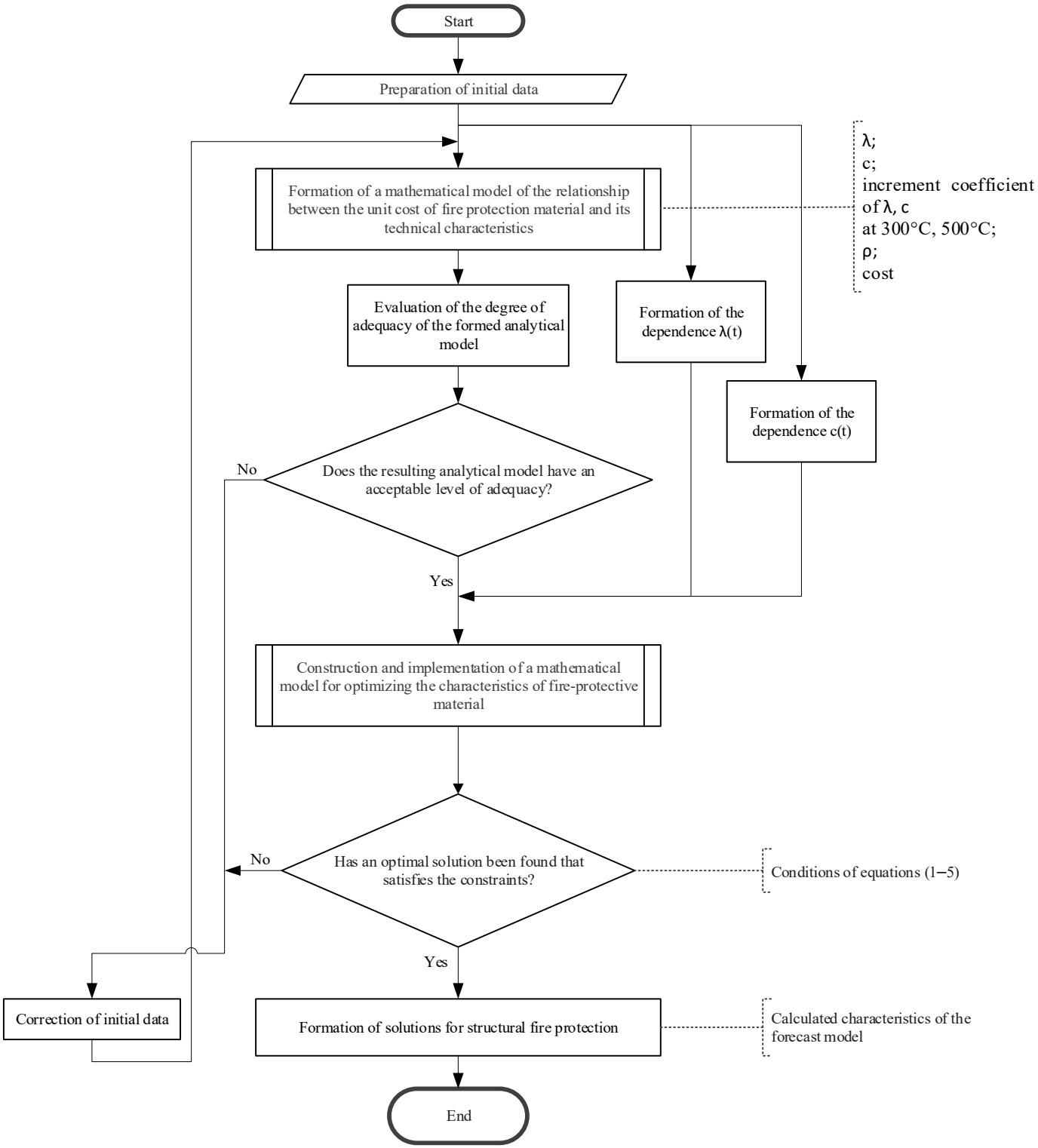


Figure 6. Block diagram of the model for calculating the cost of fire protection material.

3.1. Genetic Algorithm Procedure

The algorithm is constructed by modifying the iterative scheme developed in [33]. The flowchart is shown in Figure 7. Each design variant with fire protection is represented as an individual, whose set of genes determines its variable parameters. The individual

characteristic, i.e., the gene, is represented as a separate variable in the solution structure (the characteristic of the fire-protective material). The individual's fitness is the value of the objective function for a separate solution. In this algorithm, each individual represents a set of genes that can act as an alternative solution, that is, a sequence of analytical results. An individual's characteristic is a single gene or a single variable in the solution representation (a material characteristic). The population represents a set of alternative solutions. The fitness of an individual is the value of the predictive function for a single solution.

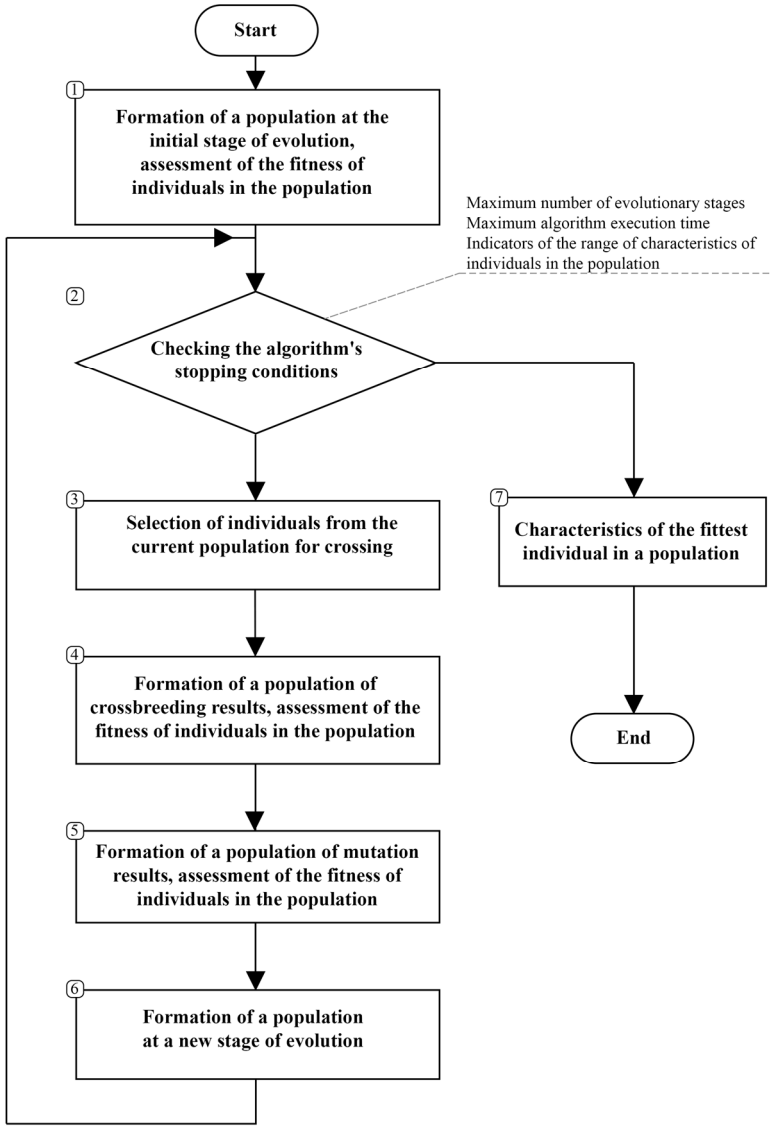


Figure 7. Block diagram of the optimization algorithm.

3.2. Implementation of the Model Using a Practical Example

The model was implemented using the example of a steel structure with a volumetric coefficient of 134 mm^{-1} under the influence of the S-mode, with a fire-protective structural material located along the perimeter of the structure. Let us consider a sample of fire-protective structural materials in the amount of 39 units that do not change their geometric characteristics during a fire. The sample includes fire protection products containing mineral wool, cement slabs, basalt, and ceramic fiber. The initial data for the model can be seen in the Supplementary Materials, based on official sources from fire protection manufacturers and also obtained based on experimental modeling. The data for some

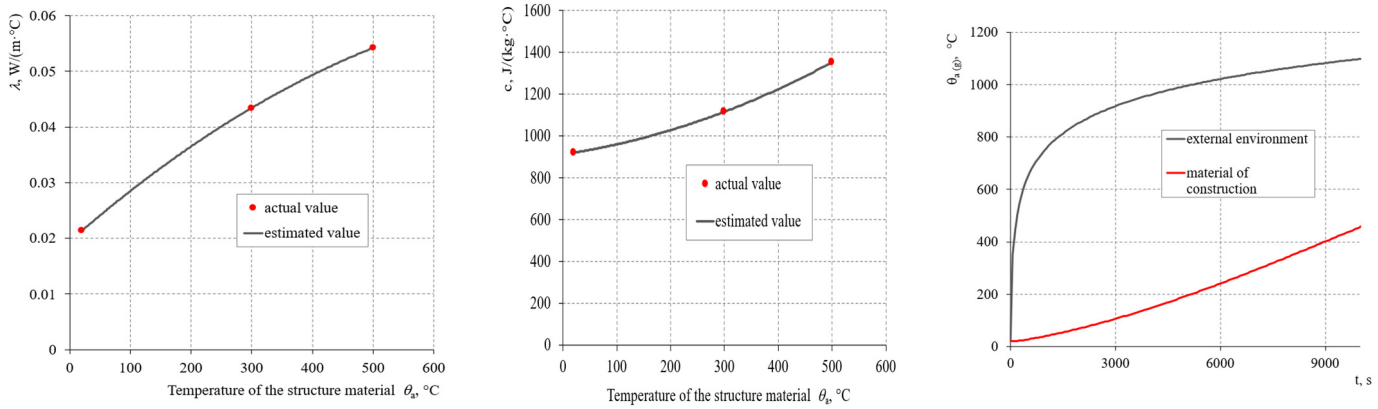
manufacturers are averaged and provided for the scale of statistics. A complete list of materials is provided in [36]. The names of the materials are not given, only their numbers.

The following constraints are considered:

1. Geometric stability of the fire protection rod system during a fire (in the model, the temperature must not reach 500 °C for 180 min).
2. The material density does not change during a fire.
3. Maximum and minimum cost constraints for the materials in the sample: \$80.00/m^2 and \$4.00/m^2, respectively.
4. The temperature on the unheated steel surface beneath the fire protection must not exceed 500 °C.

With the help of calculations using the genetic algorithm in the "Solver" add-in, it is possible to construct monotonic graphs for three reference points showing the dependence of the thermal conductivity and heat capacity coefficients of the fire-protective material on temperature up to 500 °C (Figure 5). The coefficient increments were taken as the ratios of λ at 20 °C, 300 °C, and 500 °C. Interpolation is carried out on the basis of a quadratic polynomial.

The graph in Figure 8c shows the dependence of the S-mode with a step of 60 s on time. Taking into account this dependence on the graphs of Figure 8a,b, it is possible to predict λ and c to meet the restrictions of 180 min to reach 500 °C on the unheated surface of the steel structure with fire-protective material.



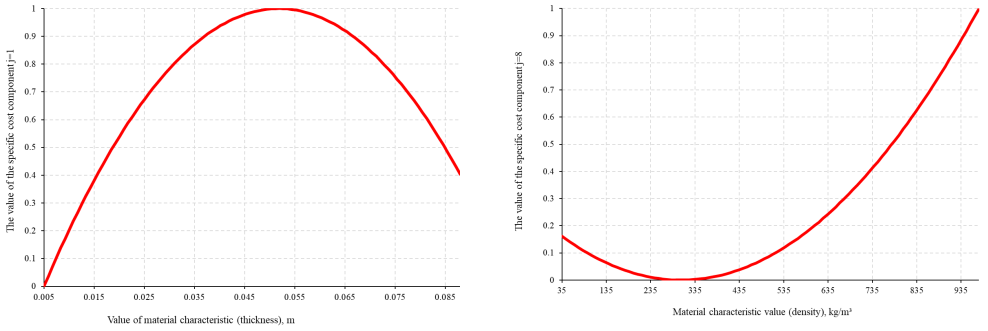
(**a**) (**b**) (**c**)

Figure 8. Dependences of parameters λ (**a**), c (**b**), and θ (**c**) for the optimal solution, obtained in the model for three support points.

The actual values of the coefficients λ and c are obtained based on the values for the reference points at 20°, 300°, and 500 °C (the data are averaged for each material). The calculated values of the coefficients λ and c are interpolation dependencies that are proposed for the design fire protection material and correspond to the hypothesis of the regularities valid for the calculation object. To a certain extent, the type of quadratic dependence will also be valid for standard fire protection materials. For example, in the ROCKWOOL Russia Group division (Technical Insulation Catalogue, issue 07.2023) [37], a quadratic dependence of λ on temperature is also proposed. The calculated value of the coefficient of determination $\left(R^{\mathrm{I}}\right)^2$ for the forecast model of the main component was 0.948 (item 1.6 in Table 5 in Figure S1 in the Supplementary Materials), the calculated coefficient of determination of the forecast model for the additional component $\left(R^{\mathrm{II}}\right)^2$ was 0.871 (item 2.6 in Table 5 in Figure S1 in the Supplementary Materials), which confirms the significance of the model and its forecast quality (relatively high degree of correspondence

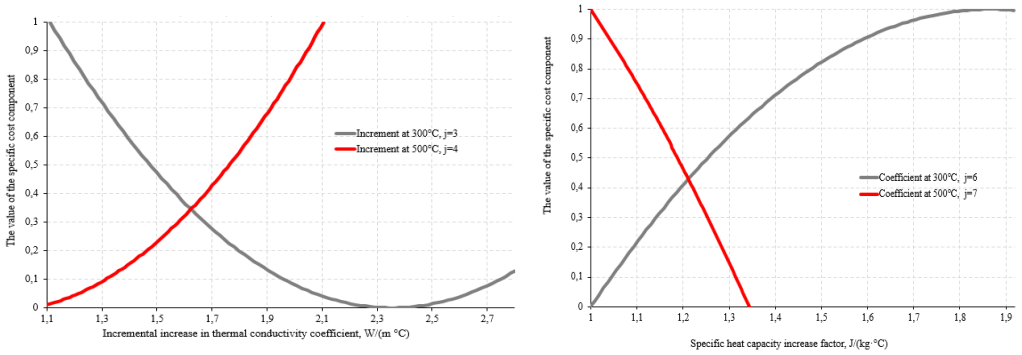
for the model data). The predicted specific cost of fire-protective structural material $\widetilde{y}$ was 6.83 \$/m^2 (Table 10, Figure S4 in the Supplementary Materials).

Figures 9–11 presents the dependences of the normalized results of the cost of the material component (column AF (y_i) in the Supplementary Materials) on each parameter of the alternative quantity ($MU_{x\,j}$, Table 1), expressed in successive measurements, obtained as a result of Min–Max normalization. All dependences are parabolic due to the quadratic polynomial of the objective function.



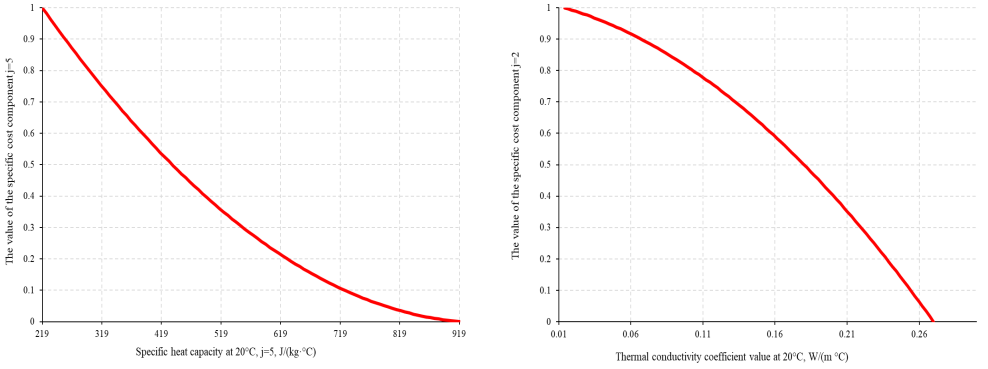
(**a**) (**b**)

Figure 9. Graphs of the dependence of the standardized component of the conditional cost: (**a**) thickness of fire-protective material and (**b**) density of fire-protective material.



(**a**) (**b**)

Figure 10. Graphs of the dependence of the standardized component of the conditional cost: (**a**) the gradual increase in thermal conductivity and (**b**) the coefficient of increment of specific heat capacity.



(**a**) (**b**)

Figure 11. Graphs of the dependence of the standardized component of the conditional cost: (**a**) on the heat capacity at 20 °C and (**b**) on the thermal conductivity coefficient at 20 °C.

3.3. Model Validation

For comparison with the reference values (Figure 8), we examined the thermal conductivity and heat capacity of the PROZASK refractory board (high-end price category, as per the Supplementary Materials). The board is a Portland cement composite reinforced with fiberglass mesh on both sides and has a protective coating on one side.

According to [6], the thermal conductivity coefficient of the PROZASK Firepanel board is 0.391 W/(mK) at 25 °C and the specific heat capacity is 1444 J/(kgK) with a board density of 1100 kg/m^3. Table 4 presents the calculated thermophysical parameters of the Pyrosafe-Austuver T and PROZASK Firepanel boards (calculated parameters are shown in italics) and the experimental parameters, according to standardized methods [6].

Table 4. The thermal characteristics of Pyrosafe-Austuver T and PROZASK panels.

T, °C	25	100	200	300
λ, W/K·m	0.17/0.257 *	0.14	0.12	0.11
C, J/kg·m	750/732 **	800/1068 **	815/1219 **	830/1164 **, 1216 ***

Note: * Values obtained on samples measuring 100 × 100 mm with a density of 1124 kg/m^3; ** the indicators obtained according to [38], *** the values were obtained from samples measuring 300 × 200 mm and 12.5 mm thick for panels with a density of 1124 kg/m^3 [16].

As can be seen in Table 4, the experimental heat capacity coefficients are virtually identical to the control points in Figure 8, whereas the thermal conductivity coefficient is 20–30% lower. For more accurate models, it is necessary to rely on standard fire tests and obtain thermophysical characteristics by solving the inverse thermal conductivity problem, as experimental studies determining the thermal conductivity of coatings at temperatures above 300 °C are difficult.

The rockwool mineral wool of the ProRox PS 960 (density 114 kg/m^3) and ProRox PS 970 (density 145 kg/m^3) brands has higher thermal conductivity values (λ300 in the range of 0.092–0.085 W/(M·K)) than the values in graph 8 (average price category according to the Supplementary Materials) [37].

Basalt fibrous materials, closest in properties to the reference values in the models in Figure 8 (with the lowest price according to the Supplementary Materials), were identified according to experimental data [39]. Table 5 presents data on the effective thermal conductivity coefficient of basalt fibers depending on temperature and density.

Table 5. The thermal conductivity values of basalt fiber.

T, °C	Thermal Conductivity, λ, W/m·K at Density, ρ		
	ρ = 80 kg/m^3	ρ = 100 kg/m^3	ρ = 120 kg/m^3
50	0.0242	0.0217	0.0209
100	0.0277	0.0263	0.0246
200	0.0374	0.0345	0.0329
300	0.0488	0.0526	0.0464

The results obtained in the model, for example, may correspond to a 60 mm thick «Izovent» basalt wool slab, with a minimum density of 120 kg/m^3, or to mats or rolls of 70 thick «Bison-70-1F» superfine basalt fiber without binder, with a density of at least 35 kg/m^3, manufactured using a stitched or knitted–stitched method, with or without a facing material. The data were taken from the manufacturers' brochures [36].

4. Limitations and Future Work

This model assumes that the geometry of the fire-retardant material does not change when exposed to high temperatures. It assumes that the material is strong and durable, and that moisture is not taken into account. Future plans include calculating the optimal density and the cost of fire-retardant plaster compositions that maintain their geometry. The model should also take into account the cost of construction and installation work, which, incidentally, will be quite similar for paints and plaster compositions (Figure 4), but may differ for structural compositions. For intumescent paints, the dependence of thermal conductivity on heat capacity will be quite complex due to the increased thickness and reduced density of the fire-retardant layer in the form of foam coke [6]. Another limitation of the model was that the steel structure could not reach a temperature of 500 °C under standard temperature conditions (Figure 2). Fire protection in the oil and gas industry requires the use of hydrocarbon combustion modes (Figure 3), and the behavior of the insulating material must be modeled specifically under these conditions.

Currently, there is a trend toward integrating artificial intelligence into classical optimization algorithms. Neural network models can approximate complex objective functions, significantly accelerating the process of finding the optimum for computationally intensive problems. In ref. [26], the authors demonstrated that for masonry studies, AI methods can reduce the error rate by approximately 80% and improve the correlation strength by approximately 30% compared to traditional formulas, with ensemble learning methods performing particularly well. Similar conclusions were reached by the authors in a study of concrete [40–42] and composite beams [43]. Therefore, future research will include the use of ensemble learning methods and the integration of calculation results into a building information model (BIM). It will be possible to calculate the cost of fire protection for structures and fire protection performance, for example, for high-rise buildings, for which the required fire resistance of structures can reach R180 and R240 min [44]. Integration with BIM platforms with appropriate scripts will also allow for visualization and additional analysis.

5. Conclusions

Thus, the parameters of the quadratic function of the dependence of the cost of purchasing fire protection material on the technical characteristics of the material were calculated using the adapted least squares method based on a given sample of examples of structural fire protection means. An assessment of the adequacy of the model was carried out based on a given sample of samples.

A mathematical model was developed that enables the calculation of the minimum cost of structural fire protection, considering temperatures reaching 500 °C on the unheated side of the steel column and 180 min of the standard fire mode.

The model is implemented using an example of a steel structure with a volumetric coefficient of 134 mm^{-1} under the influence of the S-mode, with a fire protection structural material located along the perimeter of the structure.

The calculated value of the determination coefficient R for the predictive model of the main component was 0.948. The predicted cost of the material was 6.83 $\$/m^2$. This low cost was due to the model not including component installation work. However, the practical benefit of such a model is that by changing the parameters of the cost of materials on the market, as well as adding the cost of the installation component, it is possible to estimate the optimal cost of fire-protective materials for increasing the fire resistance of structures under standard fire conditions.

Supplementary Materials: The following supporting information can be downloaded at: https://www.mdpi.com/article/10.3390/buildings16010215/s1, Figure S1: A fragment of the "Calculation" worksheet in the "Microsoft Excel" program file, corresponding to the presentation of the parameters and characteristics of the optimization model; Figure S2: A fragment of the "Calculation" worksheet in the "Microsoft Excel" program file, corresponding to the presentation of the initial data of the optimization model; Figure S3: A fragment of the "Calculation" worksheet in the "Microsoft Excel" program file, corresponding to the presentation of the initial data of the optimization model; Figure S4: A fragment of the "Calculation" worksheet in the "Microsoft Excel" program file, corresponding to the presentation of the calculated characteristics of the optimization model; Figure S5: A fragment of the worksheet "Auxiliary calculation_1" in the "Microsoft Excel" program file, corresponding to the representation of the main matrix of the systems of equations for the main calculation characteristics of the optimization model; Figure S6: A fragment of the worksheet "Auxiliary calculation_1" in the "Microsoft Excel" program file, corresponding to the representation of the matrix of systems of equations for the main calculation characteristics of the optimization model; Figure S7: A fragment of the worksheet "Auxiliary calculation_2" in the file of the program "Microsoft Excel", corresponding to the representation of the main matrix of the systems of equations for additional calculation characteristics of the optimization model; Figure S8: A fragment of the worksheet "Auxiliary calculation_2" in the "Microsoft Excel" program file, corresponding to the representation of the matrix of systems of equations for additional calculation characteristics of the optimization model; Table S1: Principles of filling cells of worksheets in the file of the program "Microsoft Excel", corresponding to the optimization model; Table S2: Initial data and parameters for the optimization model.

Author Contributions: Conceptualization, M.G.; methodology, M.G.; software, N.S.; validation, N.S. and N.K.; formal analysis, A.R.; investigation, A.R.; data curation, N.K. and A.T.; supervision, M.G.; writing—original draft, M.G. All authors have read and agreed to the published version of the manuscript.

Funding: This research was funded by the Ministry of Science and Higher Education of the Russian Federation within the framework of the state assignment No 075-03-2025-256 dated 16 January 2025, Additional agreement No 075-03-2025-256/1 dated 25 March 2025, FSEG-2025-0008.

Data Availability Statement: Data are contained within the article.

Conflicts of Interest: The authors declare no conflicts of interest.

References

1. *ISO 834-1:1999/Amd 2:2021*; Fire-Resistance Tests. Elements of Building Construction. Part 1: General Requirements. ISO: Geneva, Switzerland, 2021. Available online: https://www.iso.org/ru/standard/81661.html (accessed on 22 December 2025).
2. Džolev, I.; Kekez-Baran, S.; Rašeta, A. Fire Resistance of Steel Beams with Intumescent Coating Exposed to Fire Using ANSYS and Machine Learning. *Buildings* **2025**, *15*, 2334. [CrossRef]
3. Hassoune, M.; Kada, A.; Menadi, B.; Lamri, B.; Yessad, O.; Piloto, P.A.; Jiang, L. Performance of single and built-up I-shaped cold formed steel stud under double sided walls fire exposure. *Eng. Struct.* **2025**, *335*, 120392. [CrossRef]
4. *EN 1363-1:2020*; Fire Resistance Tests—Part 1: General Requirements. Slovenski Inštitut za Standardizacijo: Ljubljana, Slovenia, 2020. Available online: https://standards.iteh.ai/catalog/standards/cen/243adbdc-e0e0-43ac-a801-22c8e91e7f3c/en-1363-1-2020?srsltid=AfmBOookIsJU3EPvpbYwXaiZuu4oU2bhlu7zJS2dAHdgFgOOTTD04CvJ (accessed on 22 December 2025).
5. *UL 1709-2017*; Standard for Safety Rapid Rise Fire Tests of Protection Materials for Structural Steel. Underwriters Laboratories Inc. (UL): Northbrook, IL, USA, 2017. Available online: https://docs.cntd.ru/document/550713257 (accessed on 22 December 2025).
6. Gravit, M.; Dmitriev, I.; Shcheglov, N.; Radaev, A. Oil and Gas Structures: Forecasting the Fire Resistance of Steel Structures with Fire Protection under Hydrocarbon Fire Conditions. *Fire* **2024**, *7*, 173. [CrossRef]
7. *GOST R 53293-2009*; Fire Hazard of Substances and Materials, Materials, Substances and Means. RUNORM: Moscow, Russia, 2009. Available online: https://runorm.com/catalog/102/828617 (accessed on 22 December 2025).
8. *ASTM E119*; Standard Test Methods for Fire Tests of Building Construction and Materials. ASTM International: West Conshohocken, PA, USA, 2022. Available online: https://www.astm.org/e0119-00a.html (accessed on 29 January 2024).

9. *EN 1991-1-2*; Eurocode 1: Actions on Structures—Part 1–2: General Actions—Actions on Structures Exposed to Fire. European Union: Brussels, Belgium, 2002. Available online: https://www.phd.eng.br/wp-content/uploads/2015/12/en.1991.1.2.2002.pdf (accessed on 25 October 2023).
10. *BS EN 13381-4-2013*; Test Methods for Determining the Contribution to the Fire Resistance of Structural Members—Part 4: Applied Passive Protection to Steel Members. European Union: Brussels, Belgium, 2013. Available online: https://knowledge.bsigroup.com/products/test-methods-for-determining-the-contribution-to-the-fire-resistance-of-structural-members-applied-passive-protection-products-to-steel-members (accessed on 22 December 2025).
11. ETAG 018-2013/Guideline for European Technical Approval of Fire Protective Products. Part 1: General. Available online: https://www.eota.eu/sites/default/files/uploads/ETAGs/etag-018-part-1-april-2013.pdf (accessed on 22 December 2025).
12. Pereira, D.; Fonseca, E.M.M.; Osório, M. Computational Analysis for the Evaluation of Fire Resistance in Constructive Wooden Elements with Protection. *Appl. Sci.* **2024**, *14*, 1477. [CrossRef]
13. Bolina, F.L.; Rodrigues, J.P.C. Temperature field of composite steel and concrete slabs in fire situation. *Rev. IBRACON Estrut. Mater.* **2024**, *17*, e17208. [CrossRef]
14. Ma, C.; Gernay, T. Numerical analysis of full-scale structural fire tests on composite floor systems. *Fire Saf. J.* **2024**, *146*, 104182. [CrossRef]
15. Kodur, V.; Raut, N. A simplified approach for predicting fire resistance of reinforced concrete columns under biaxial bending. *Eng. Struct.* **2012**, *41*, 428–443. [CrossRef]
16. Buchanan, A. The Challenges of Predicting Structural Performance in Fires. *Fire Saf. Sci.* **2008**, *9*, 79–90. [CrossRef]
17. Venkatachari, S.; Kodur, V.K.R. Modeling parameters for predicting the fire-induced progressive collapse in steel framed buildings. *Resilient Cities Struct.* **2023**, *2*, 129–144. [CrossRef]
18. Chaudhary, R.K.; Gernay, T.; Van Coile, R. Cost-optimization based target reliabilities for design of structures exposed to fire. *Resilient Cities Struct.* **2024**, *3*, 20–33. [CrossRef]
19. Rashid, H.A.; Al-Juboori, O.A.; Mahjoob, A.M.R. Genetic Algorithms in Construction Project Management: A Review. *Solid State Technol.* **2021**, *64*, 5193–5213.
20. Srimathi, K.R.; Padmarekha, A.; Anandh, K.S. Automated construction schedule optimisation using genetic algorithm. *Asian J. Civ. Eng.* **2023**, *24*, 3521–3528. [CrossRef]
21. Benaddi, F.Z.; Boukhattem, L.; Tabares-Velasco, P.C. Multi-objective optimization of building envelope components based on economic, environmental, and thermal comfort criteria. *Energy Build.* **2024**, *305*, 113909. [CrossRef]
22. Wu, C.; Pan, H.; Luo, Z.; Liu, C.; Huang, H. Multi-objective optimization of residential building energy consumption, daylighting, and thermal comfort based on BO-XGBoost-NSGA-II. *Build. Environ.* **2024**, *254*, 111386. [CrossRef]
23. Olekhnovich, Y.A.; Radaev, A.E. Justification of the combination of standard values of characteristics of materials of layers in the enclosing structure based on quadratic optimization. *Bull. MGSU* **2025**, *20*, 193–214. [CrossRef]
24. Olekhnovich, Y.A. Methodology for Substantiating the Characteristics of Enclosing Structures of Residential Buildings Based on Energy Efficiency Criteria. Diss. Candidate of Engineering Sciences, SPbPU, St. Petersburg. 2025. Available online: https://www.spbstu.ru/dsb/09bb-thesis.pdf (accessed on 22 December 2025).
25. Memarzadeh, A.; Shahmansouri, A.; Nematzadeh, M.; Gholampour, A. A review on fire resistance of steel-concrete composite slim-floor beams. *Steel Compos. Struct.* **2021**, *40*, 13–32. [CrossRef]
26. Memarzadeh, A.; Nazari, A.; Sabetifar, H.; Nematzadeh, M. Advanced predictive modeling for masonry walls: A comparative study of six AI models and existing empirical formulas. *Results Eng.* **2025**, *28*, 107634. [CrossRef]
27. Li, Y. Optimization Method of Building Structure Design Based on Genetic Algorithm. The 5th International Conference on Multi-modal Information Analytics (MMIA). *Procedia Comput. Sci.* **2025**, *262*, 1344–1351. [CrossRef]
28. Yavan, F.; Maalek, R. Reliability-Constrained Structural Design Optimization Using Visual Programming in Building Information Modeling (BIM) Projects. *Appl. Sci.* **2025**, *15*, 1025. [CrossRef]
29. *SP 20.13330*; Loads and Impacts. Ministry of Construction Industry, Housing and Utilities Sector of the Russian Federation: Moscow, Russia, 2016.
30. *SP 16.13330.2017*; Steel Structures. Ministry of Construction Industry, Housing and Utilities Sector of the Russian Federation: Moscow, Russia, 2017.
31. *EN 1993-1-2:2005*; Eurocode 3: Design of Steel Structures. Part 1–2: General Rules—Structural Fire Design. European Committee for Standardization: Brussels, Belgium, 2005. Available online: https://www.phd.eng.br/wp-content/uploads/2015/12/en.1993.1.2.2005.pdf (accessed on 22 December 2025).
32. Barthelemy, B.; Kruppa, J. Fire Resistance of Building Structures—M.: Stroyizdat, 1985. 216p. Available online: https://fireman.club/literature/ognestojkost-stroitelnyh-konstrukczij-1985/ (accessed on 22 December 2025).
33. National Standard of Russia GOST R 53295-2009 Fire Retardant Compositions for Steel Constructions. General Requirement. Method for Determining Fire Retardant Efficiency. Available online: https://docs.cntd.ru/document/1200071913 (accessed on 22 December 2025).

34. Alekseytsev, A.V.; Kurchenko, N.S. Searching the rational parameters of bar steel structures based on adaptive evolutionary model. *Struct. Mech. Eng. Constr. Build.* **2011**, *3*, 7–14.
35. Shadrina, N.I.; Berman, N.D. *Solving Optimization Problems in Microsoft Excel 2010: A Tutorial*; Vikhtenko, E.M., Ed.; Publishing House of Pacific State University: Khabarovsk, Russia, 2016; 101p, ISBN 978-5-7389-1886-5.
36. Bazukova, E.; Vankov, Y.; Gaponenko, S.; Smirnov, N. Study of thermal conductivity coefficient of basalt fiber insulation at various temperature conditions. *Vestn. IGEU* **2021**, *4*, 15–24. [CrossRef]
37. Gravit, M.V.; Nedryshkin, O.V.; Petrochenko, M.V. *Structural Methods for Increasing the Fire Resistance of Load-Bearing Steel Structures [Electronic Resource]*; study guide; Peter the Great St. Petersburg Polytechnic University, Civil Engineering Institute, Department of "Construction of Unique Buildings and Structures": St. Petersburg, FL, USA, 2016. [CrossRef]
38. Mitsel, A.A. *Optimization Methods*; Mitsel, A.A., Shelestov, A.A., Romanenko, V.V., Eds.; Part 2: Tutorial; Publishing House of Tomsk. State University of Control Systems and Radioelectronics: Tomsk, Russia, 2022; 350p.
39. *State Standard 23630.1-79*; Plastics Method for the Determination of Thermal Capacity. USSR State Committee for Standards: Moscow, Russia, 1979. Available online: https://docs.cntd.ru/document/1200018701 (accessed on 22 December 2025).
40. Technical Insulation Catalog of ROCKWOOL Group. Available online: https://rwl.ru/files/rw/documents/katalog-tekhnicheskoy-izolyatsii%20-%2020227.pdf (accessed on 22 December 2025).
41. Motsa, S.M.; Stavroulakis, G.E.; Drosopoulo, G.A. A data-driven, machine learning scheme used to predict the structural response of masonry arches. *Eng. Struct.* **2023**, *296*, 116912. [CrossRef]
42. Nematzadeh, M.; Nazari, A.; Tayebi, M. Post-fire impact behavior and durability of steel fiber-reinforced concrete containing blended cement–zeolite and recycled nylon granules as partial aggregate replacement. *Arch. Civ. Mech. Eng.* **2021**, *22*, 5. [CrossRef]
43. Rezaeicherati, F.; Arabkhazaeli, A.; Memarzadeh, A.; Naghipour, M.; Vahedi, A.; Nematzadeh, M. Experimental study of post-fire bond behavior of concrete-filled stiffened steel tubes: A crucial aspect for composite structures. *Structures* **2024**, *62*, 106203. [CrossRef]
44. Code of Practice 477.1325800.2020 Highrise Buildings and Complexes. Fire Safety Requirements. Available online: https://docs.cntd.ru/document/564612859 (accessed on 22 December 2025).

Disclaimer/Publisher's Note: The statements, opinions and data contained in all publications are solely those of the individual author(s) and contributor(s) and not of MDPI and/or the editor(s). MDPI and/or the editor(s) disclaim responsibility for any injury to people or property resulting from any ideas, methods, instructions or products referred to in the content.